Solar-Terrestrial Physics. 2019. Vol. 5. Iss. 1. P. 3–10. DOI: 10.12737/stp-51201901. © 2019 I. Zhivanovich, A. Riehokainen, A.A. Solov'ev, V.I. Efremov. Published by INFRA-M Academic Publishing House
Original Russian version: I. Zhivanovich, A. Riehokainen, A.A. Solov'ev, V.I. Efremov, published in Solnechno-zemnaya fizika. 2019. Vol. 5. Iss. 1. P. 4–12. DOI: 10.12737/szf-51201901. © 2019 INFRA-M Academic Publishing House (Nauchno-Izdatelskii Tsentr INFRA-M)

QUASI-PERIODIC OSCILLATIONS OF SMALL-SCALE MAGNETIC STRUCTURES AND A SPECIFIC METHOD FOR MEASURING THE DIFFERENTIAL ROTATION OF THE SUN

I. Zhivanovich
Central Astronomical Observatory RAS at Pulkovo, Saint Petersburg, Russia, ivanzhiv@live.com
V.V. Sobolev Astronomical Institute, Saint Petersburg State University, Saint Petersburg, Russia, ivanzhiv@live.com
A. Riehokainen
Faculty of Physics and Astronomy, University of Turku, Finland, alerie@utu.fi
A.A. Solov'ev
Central Astronomical Observatory RAS at Pulkovo, Saint Petersburg, Russia, solov.a.a@mail.ru
Kalmyk State University, Elista, Russia, solov.a.a@mail.ru
V.I. Efremov
Central Astronomical Observatory RAS at Pulkovo, Saint Petersburg, Russia, slavae_sun@mail.ru

Abstract. The SDO/HMI data with an angular resolution of 1 arcsec have been used to explore the differential rotation on the Sun, using an original p2p effect on the basis of the movement of small-scale magnetic structures in the photosphere of the Sun. It is shown that a stable p2p artifact inherent in the SDO/HMI data can be an effective tool for measuring the speed of various tracers on the Sun. In particular, in combination with the Fourier analysis, it allows us to investigate the differential rotation of the Sun at various latitudes. The differential rotation curve obtained from the SDO/HMI magnetograms by this method is in good agreement with the curves obtained earlier from ground-based observations.

Keywords: solar physics, small-scale magnetic structures, differential rotation of the Sun.

INTRODUCTION

The study of quasi-periodic oscillations of different structures on the Sun in active regions and outside them plays a key role in studying physical parameters of the solar atmosphere [Foullon et al, 2009; Yuan et al., 2011]. Solar oscillations with a period from 3 to 10 min are well known. They can be interpreted as propagation of MHD waves along magnetic tubes in active solar formations [Thomas et al., 1984; Chelpanov et al., 2015, 2016]. In addition, oscillations with periods from 20–40 min to tens of hours have been found in the power spectra of solar magnetic elements: sunspots, filaments, and faculae [Efremov et al., 2010; Solov'ev, Kirichek, 2014; Smirnova et al., 2013; Kolotkov et al., 2017].

Regular periodic processes observed on the Sun give us a reliable time standard. Regular processes are not only harmonic oscillations, but also any process in which the spectrum of the fundamental mode is well-defined and stable. One of such processes, which is called the p2p effect, occurs in all observations, when discrete detectors such as CCD are employed. In particular, this effect manifests itself in SDO/HMI data (SDO – Solar Dynamics Observatory, HMI – Helio-seismic and Magnetic Imager) [Scherrer et al., 2012].

This is a parasitic effect, i.e. an artifact, but it is stable, and therefore we can use this artifact as an effective tool to study various time processes on the Sun. We exploit the p2p artifact as a method for determining the speed of tracers on the solar surface.

1. THE P2P ARTEFACT

The p2p artifact manifests itself as follows: an extreme reading (intensity, magnetic field, etc.) gradually moves from one pixel to the adjacent one and for a time is projected on the boundary between two pixels. In the pixel, in which a maximum intensity has recently been detected, a minimum intensity is recorded. Information is, however, still being read from this pixel and provides a local minimum at the signal level. Then, the extreme reading proceeds to the next pixel, and the maximum value is restored. The regular transition of the extremal point of a distributed object from one pixel of a discrete matrix to another yields a false periodicity in the signal. This effect is called p2p (pixel-to-pixel) [Efremov et al., 2010, 2018]. It is obvious that in continuous receivers (e.g., photographic planes) such an artifact cannot appear.

The p2p effect is described in more detail by Efremov et al. [2018]. The size of the area with the extreme reading of the magnetic field is generally comparable to or smaller than the size of a pixel. In Figure 1, the top panel shows a typical time series obtained for the magnetic field strength. The bottom panel presents the time series of the horizontal coordinate of the point with an extreme magnetic field value on the matrix.

The bottom panel of Figure 1 (see also Figure 2) clearly shows a stepwise structure. The extreme value seems not to shift along the matrix (in fact, this point moves, but its movement is invisible due to the finite size of the pixel of the matrix). Then there is an abrupt transition of the extreme value to the next pixel. It is significant that the width of the step corresponds to a period of the p2p artifact. Figure 2 presents larger (smaller) fragments of the time series from Figure 1 for better visualization of the p2p effect. We can see that the mean period of time variations in the magnetic field

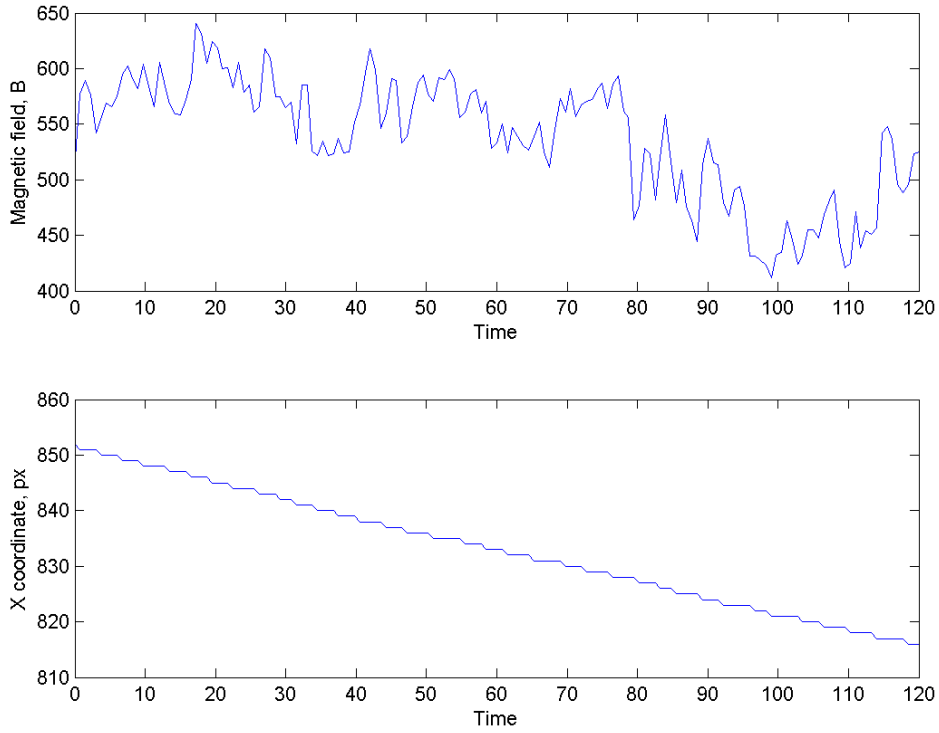

Figure 1. Time extreme magnetic field value (top panel) and time series of the *x* coordinate of this point (bottom panel). The vertical line separates the fragment shown in a larger size in Figure 2

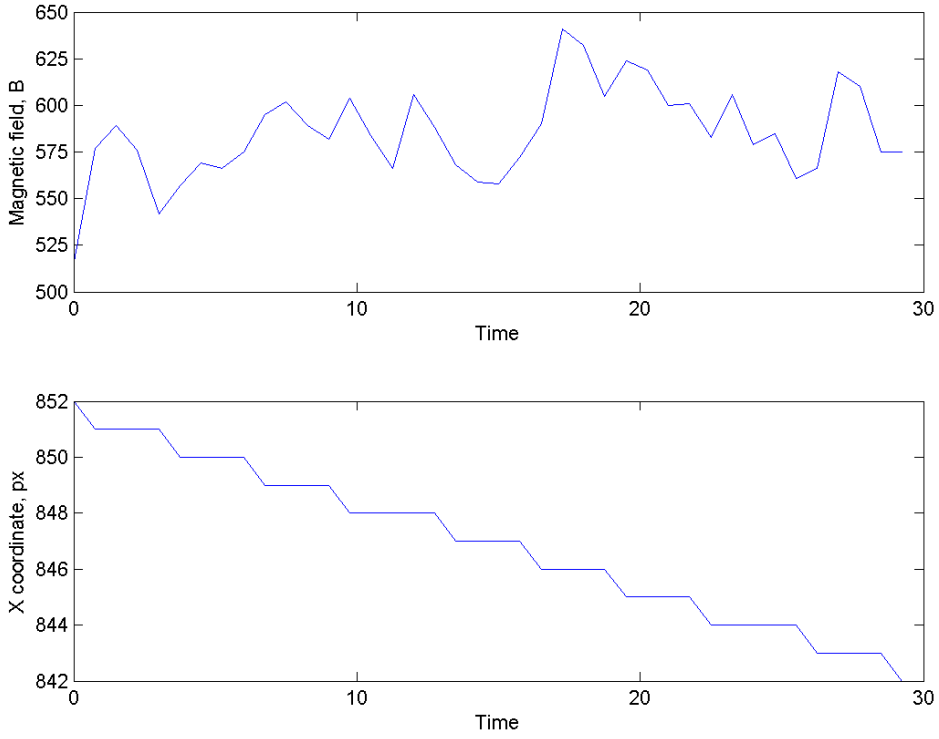

Figure 2. Fragments of time series of extreme magnetic field values (top panel) and *x* coordinate of this point (bottom panel)

(top panel in Figure 2) corresponds to the mean width of the steps (bottom panel in Figure 2).

Of course, the p2p effect can be observed not only for the horizontal coordinate. It manifests itself in both the coordinates as shown in Figure 3. The horizontal direction of the SDO/HMI matrix corresponds to the latitude; the vertical one, to the longitude.

Referring to Figure 3, the velocity of travel of the p2p artifact along the vertical coordinate (meridional component) is 1.5 pixel per hour. For the horizontal component (when an object is moving along a circle of latitude), its velocity is about 20 pixels per hour. Thus, the velocity of travel of the p2p artifact along the meridian (for a given longitude) is much lower than that along a given latitude. We therefore use only the horizontal component of the p2p artifact in this paper.

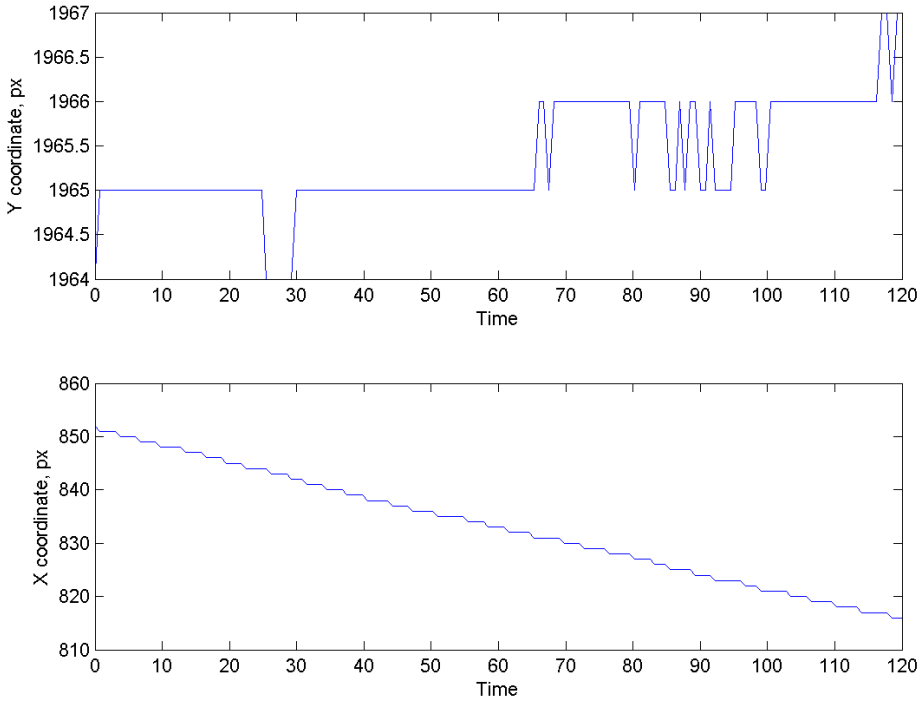

Figure 3. Both directions of the p2p effect: the top panel is the longitudinal component; the bottom panel is the latitudinal component

2. PERIOD OF THE P2P ARTIFACT AND A CURVE OF THE DIFFERENTIAL ROTATION OF THE SUN

2.1. Observational data

In this work, we have used SDO/HMI data with a spatial resolution of 1″. This allows us to deal with small-scale (an angular size from 5 to 10″) magnetic structures (Figure 4). We chose small-scale magnetic structures such that the magnetic field in them was within 200–1000 G. These structures were used as markers in constructing a curve of the differential rotation of the Sun. We utilized two time series obtained from SDO/HMI data for June 27, 2015 at the following intervals:

- 14:00:00–16:00:00 UT;
- 10:00:00–12:00:00 UT.

In addition, we used three unit large stable sunspots:

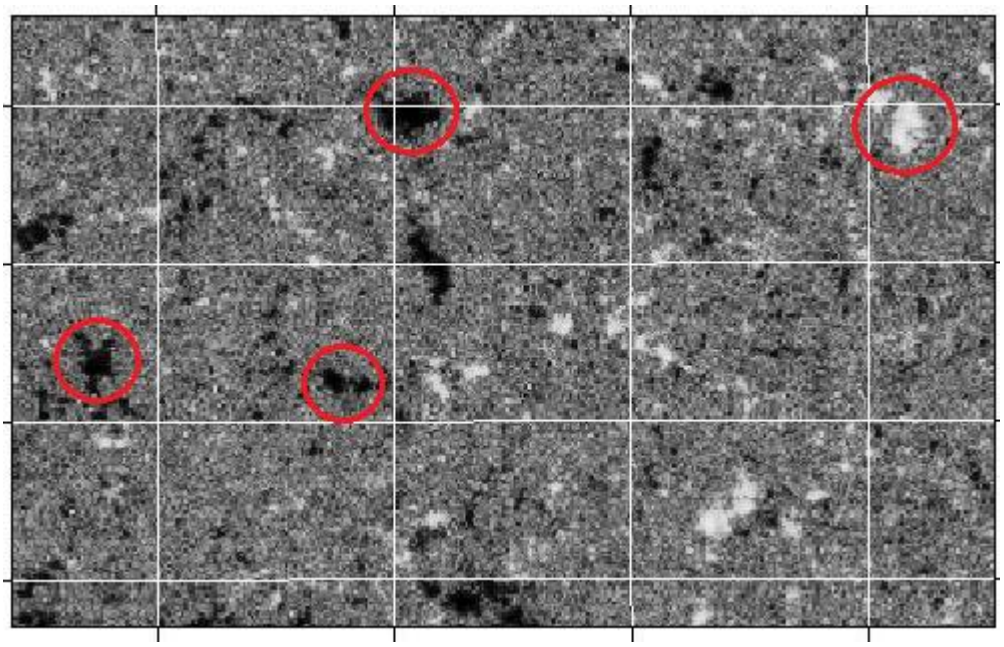

Figure 4. Fragment of an SDO/HMI magnetogram with small-scale magnetic structures (marked with red circles)

- June 26, 2013, 05:12:00–07:12:00 UT, NOAA 11777;
- January 18, 2013, 14:36:00–16:36:00 UT, NOAA 11658;
- August 05, 2013, 21:48:00–23:48:00 UT, NOAA 11809.

All the SDO/HMI data were taken with a time resolution of 45 s because the period of the p2p artifact is 3–7 min. Thus, the time cadence of 45 s enables us to reliably identify the p2p artifact. Note that, along with the temporal resolution of 45 s, there are other time cadences (12 min and 1 hr), but with them the p2p artifact cannot be identified because its period becomes smaller than the sampling increment of the time series.

The accuracy of measurements of the magnetic field strength for HMI/SDO is 10 G. At the same time, the variance of magnetic field variations in Figures 1, 2 is less than 10 G. As mentioned above, the p2p-artifact-induced magnetic field variations under study are not in fact a change in the magnetic field structure, but are associated with discreteness of a receiver (for SDO/HMI data, CCD matrix). Thus, although the accuracy in measurements of the magnetic field strength and the variance of the magnetic field variations are similar, the stable behavior of the p2p artifact period allows us to separate it from noise waves. There were, however, cases when the width of a step was unstable and varied during observation. In these cases, the noise component deadened the p2p artifact. We ignore such unstable objects in our study. The main criterion for selecting the small-scale structures in this paper is exactly the stability of the width of the steps observed in the time series of the *x* coordinate of the extreme point (bottom panels in Figures 1, 2).

Note that in both the time intervals used in this work we include only various small-scale magnetic structures, i.e. we do not use twice the objects that fall into the areas of interest during the specified time intervals.

2.2. Construction of time series for points of extreme magnetic field values

To construct time series of points of extreme values, in the solar disk we selected a region located near the central meridian (10°–15° from the central meridian) and near the apparent equator (an off-set distance of 60° at most). This region on the matrix was divided into strips of 20 pixels wide. In each of these strips, we chose the most stable and strong small-scale magnetic structure. For all strips obtained for the magnetograms considered, we constructed time series of the extreme magnetic field values and vertical and horizontal coordinates of a point with an extreme value on the matrix. The coordinates were used as a marker for stability of the position of the selected small-scale structure. At a stable position of the magnetic structure, jumps of the vertical coordinate of the extreme point during observations should not exceed 1–2 pixels. The horizontal coordinate clearly reflects the stepwise structure. For all the objects of interest, we selected time intervals, where they were stable. In some cases, however, the magnetic elements were unstable, i.e. variations of the extreme point coordinates exceeded 5–10 or more pixels.

There may be different causes of this instability: dissipation of a small-scale magnetic structure, emergence of a new magnetic flux in the selected region, etc. We omitted such magnetic structures from consideration.

Eventually we selected and used 120 different stable small-scale magnetic structures, for which lengths of time series ranged from 1 to 2 hrs.

2.3. The p2p period and other periods in the range from 3–5 to 30–40 min

For each selected small-scale magnetic structure, we found typical periods of the p2p artifact from the time series of the *x* coordinate by averaging widths of steps. This averaging is necessary because, despite the stable nature of the magnetic element, small changes in the position of the extreme point of the magnetic field structure were still observed due to processes occurring in the environment such as, in particular, the convective motion of granulation. In the time series of the *x* coordinate, these small fluctuations will cause a change in the width of steps (lengthening or shortening).

The next stage was to obtain all the observed periods of magnetic field fluctuations contained in the observed time series of the extreme magnetic field values. To these time series we applied the fifth-order Morlet wavelet and the Fourier transform. Figure 5 shows a typical wavelet spectrum and Figure 6 depicts a Fourier spectrum for the magnetic structure situated at the 9.3° latitude. As shown in Figure 5, *c*, the shorter period of 12.4 min revealed by the wavelet analysis is below the significance level, whereas the longer period of 49.6 min is above the significance level. Figure 6 presents the following periods: 3.4, 4.1, 4.8, 6, 8.6, and 20 min.

It can be seen (Figures 5, 6) that the Fourier spectrum has a better frequency resolution than the wavelet spectrum.

Since, using the wavelet transform we cannot distinguish between periods of the p2p artifact and 3–10 min oscillations generated by MHD-wave propagation along magnetic field lines, we employed the Fourier method to identify all periods for each of the objects of interest.

The identified periods can be divided into three groups: 1) periods of the p2p artifact (2–8 min); 2) periods caused by MHD-wave propagation (3–10 min); 3) periods of low-frequency oscillations (10–40 min), the physical nature of which can be explained both as the influence of granulation [Thomas et al., 1984] and as the manifestation of eigenoscillations of magnetic structures as whole objects [Efremov et al., 2010, 2018; Smirnova et al., 2013; Solov'ev, Kirichek, 2014].

The SDO/HMI data have a spatial resolution of 1″, and the resolution of the CCD matrix is 4096×4096 pixels. This gives us periods of the p2p artifact from 2 to 8 min,

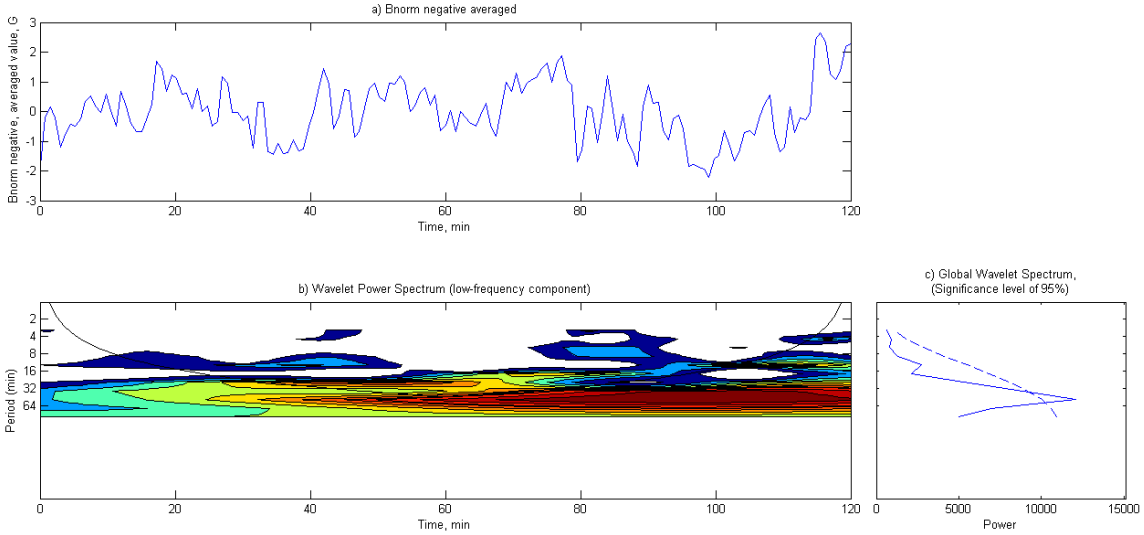

Figure 5. Time series of extreme magnetic field values (*a*) in a small-scale magnetic structure situated at a latitude of 9.3°, and its wavelet spectra (*b*, *c*). The dashed line (*c*) indicates the significance level

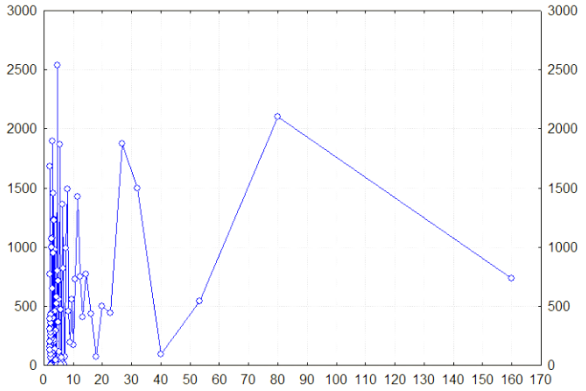

Figure 6. Fourier spectrum of the time series of the extreme magnetic field values in the small-scale magnetic structure situated at the 9.3° latitude. On the X-axis is the number of frames and to find the period, this value should be multiplied by 0.75

which falls within the range of known 3–5 min oscillations [Thomas et al., 1984]. The periods of both the types reveal themselves in magnetic field variations of the structures under study. There arises a problem of how to distinguish between these two closely related types of oscillations. Fortunately, this problem can be solved. The fact of the matter is that the time series of the *x* coordinate, in contrast to those of the magnetic field, do not contain 3–10 min periods caused by convection, but contain only periods produced by the p2p effect. This makes it possible to find typical p2p periods for each magnetic structure and separate periods of the p2p artifact from the 3–10 min periods, caused by MHD-wave propagation. The difference in the physical nature of these two types of oscillations makes itself evident also in the fact that the artifact period has a pronounced dependence on the latitude of an object, whereas for the periods of the oscillations induced by wave propagation there is no pronounced latitude dependence. This effect is well illustrated by Figure 7. The top panel shows the distribution of 3–10 min oscillations. As we can see, these periods do not depend on heliolatitude. The bottom panel shows the distribution of p2p periods having a pronounced heliolatitude dependence. This allows us to clearly distinguish between periods of these two groups.

2.4. The relation of the p2p angular velocity

We used the p2p periods to estimate the velocity of the differential rotation of the Sun. These periods can be converted into units of angular velocity (deg/day) as follows:

- the length of the circle of equal latitudes is calculated from the formula $l_\theta=2\pi R_0\cos\theta$, where l_θ is the length of the circle of equal latitudes; $R_0$is the solar radius, km; θ is the latitude of a small-scale structure;
- the pixel size in kilometers for any latitude is calculated from $R_0/sizePX = x/1\text{pixel}$, where x is the pixel size in kilometers; *sizePX* is the solar disk radius on the matrix in pixels (1872 pixels);
- now, when the length of the circle of equal latitudes and the size of one pixel in kilometers are known, the relationship between the scale of the solar surface in kilometers and the scale of an image on the matrix in pixels can be obtained by the formula $\beta=360x/l_\theta$, where β is the scale of the image on the matrix in pixels;
- finally, we can find the angular velocity Ω, deg/day, using the artifact period P_{p2p}: $\Omega=24$ [h] 60 [min] β/P_{p2p}.

2.5. The differential rotation of the Sun

We have obtained two angular velocity distributions: the first one was calculated from the mean width of steps in the time series of the *x* coordinate (top left panel in Figure 8); the second, from the period obtained from

the Fourier spectrum (top right panel in Figure 8). The data (including the source) from which we obtained the differential rotation distributions presented in Figure 8, as well as the approximation coefficients in use are listed in Table. For these distributions, analytical approximations were made using the formula proposed by Zirin [1988]:

$$\Omega = A - B\sin^2\theta - C\sin^4\theta. \quad (1)$$

Here Ω is the velocity of the differential rotation, deg/day; θ is the latitude; A, B, C are the approximation coefficients.

The differential rotation is a regular and stable process, therefore to study it we had to choose the most stable small-scale magnetic structures. We have selected 25 most stable small-scale magnetic structures of 120, such that the width of steps in the time series of the x coordinate does not exceed two pixels. The result is shown in Figure 8. The obtained distribution of the differential rotation velocity and the approximating distribution are symmetric about the equator; we therefore preferred constructing the distributions in the latitude range from 0° to 50°.

The discrepancy between the curves of the differential rotation velocity in the equatorial region is likely to be due to the fact that the classical curves were obtained for sunspots, the number of which near the solar equator was small.

If we construct such distributions for all the 120 initially selected objects, the result will be exactly the same, but the variance of the distributions will increase approximately 2.7 times. This suggests that the deviations observed in motions of the small magnetic elements under study are random and should be attributed largely to granulation effects.

CONCLUSIONS

1. Initially, we tried to adopt the above method of studying the differential rotation of the Sun to sunspots. It turned out, however, that this method yields a low accuracy for sunspots because in central parts of the sunspots, where the magnetic field is more or less uniform, the position of the extreme reading of the magnetic field strength experiences large random fluctuations. As a result, the error in determining the position of the maximum reading is not less than several pixels. In contrast, for small-scale magnetic structures the error in determining the position of the extreme value is usually less than 1–2 pixels. For this reason, to study the differential rotation of the Sun we used only small-scale magnetic structures.

2. We have shown that the stable p2p artifact inherent in SDO/HMI data in combination with the Fourier analysis is an efficient tool for measuring the speed of various tracers on the Sun.

3. Curves of the differential rotation, obtained from small-scale magnetic structures, using the p2p effect from SDO/HMI data, coincide with the curves previously derived from ground observations. An advantage of this method is that small-scale structures are uniformly distributed over the solar disk. Another advantage of this method is that to obtain a result we can use data for 1–2 hr, not for several days of observation. The p2p-artifact period (3–7 min) fits into the given time interval 10–20 times, which suggests its sufficiently precise determination.

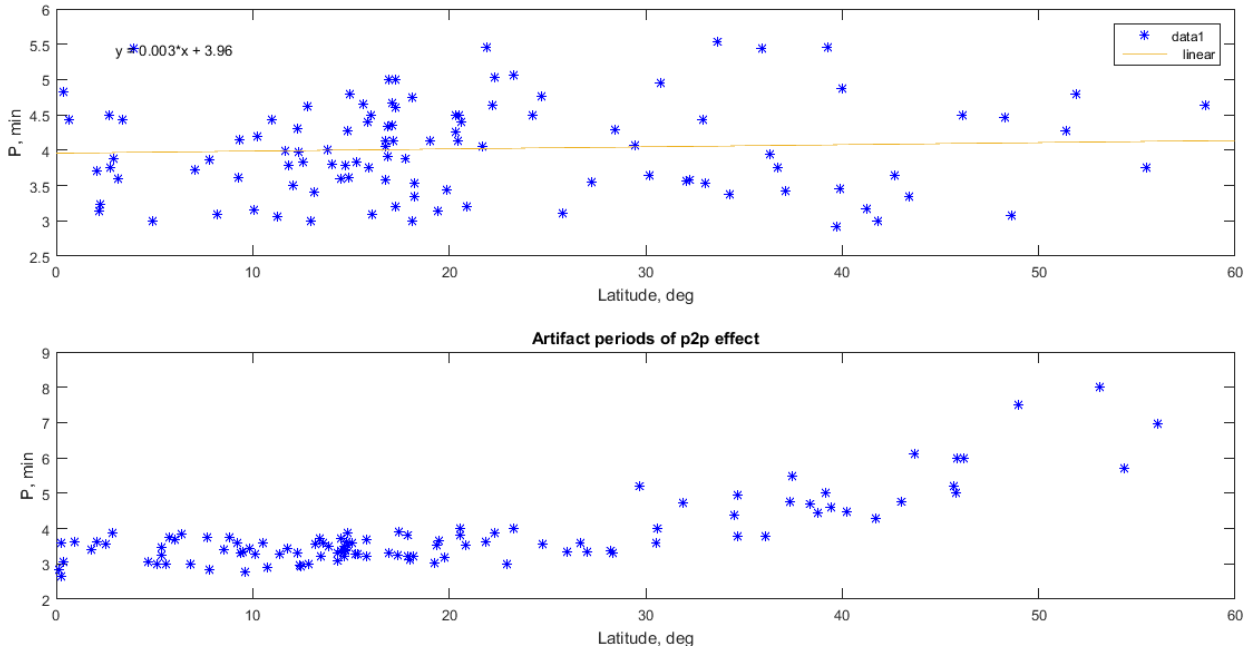

Figure 7. Distribution of 3–10 min oscillations (top panel) and periods of the p2p artifact (bottom panel) as a function of heliolatitude

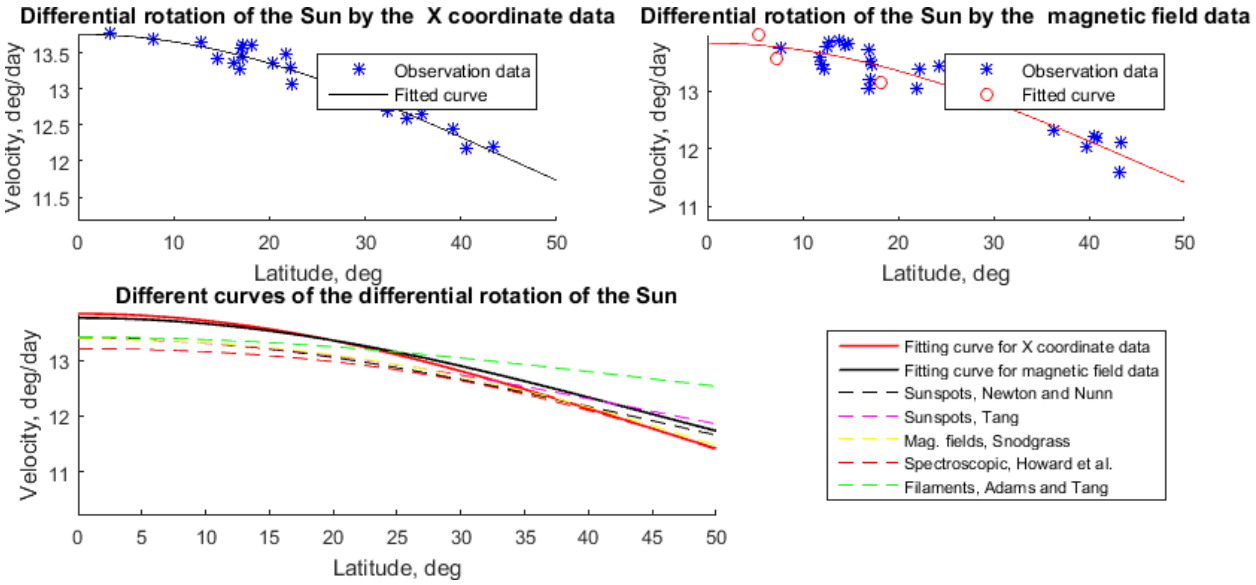

Figure 8. Differential rotation of the Sun. The circles at the top right panel mark velocities of the differential rotation of the Sun, obtained by the classical method using sunspots

Approximation coefficients in use

Data	*A*	*B*	*C*	Source
sunspots	14.38	2.96	0	Newton and Sunn [1951])
sunspots	14.37	2.60	0	Tang [1981]
magnetic field	14.37	2.30	1.62	Snodgrass [1983]
spectroscopy	14.19	1.70	2.36	Howard et al. [1983]
faculae	14.4	1.5	0	Adams, Tang [1977]
x coordinate	14.7	3.39	0	this work
magnetic field	14.8	4.115	0	this work

We express our sincere gratitude to the SDO team for the opportunity to use high-resolution material. This work was supported by RFBR grants (projects No. 18-02-00168, 18-32-00555). A. Solovyev thanks the Russian Science Foundation (Project No. 15-12-20001) for the support.

REFERENCES

Adams W., Tang F. Differential rotation of short-lived solar filaments. *Solar Phys*. 1977, vol. 55, iss. 2, pp. 499–504. DOI: 10.1007/BF00152590.

Chelpanov A.A., Kobanov N.I., Kolobov D.Y. New method to measure the tracer's speed on the Sun. *Astron. Rep*. 2015, vol. 59, iss. 11, pp. 968–973, DOI: 10.1134/S1063772915090036.

Chelpanov A.A., Kobanov N.I., Kolobov D.Y. Influence of the magnetic field on oscillation spectra in solar faculae. *Solar Phys*. 2016, vol. 291, iss. 11, pp. 3329–3338. DOI: 10.1007/ s11207-016-0954-6.

Efremov V.I., Parfinenko L.D., Solov'ev A.A. Investigation of long-period oscillations of sunspots with ground-based (Pulkovo) and SOHO/MDI data. *Solar. Phys*. 2010, vol. 267, pp. 279. DOI: 10.1007/s11207-010-9651-z.

Efremov V.I., Solov'ev A.A., Parfinenko L.D., Riehokainen A., Kirichek E., Smirnova V.V., Varun Y.N., Bakunina I., Zhivanovich I. Long-term oscillations of sunspots and a special class of artifacts in SOHO/MDI and SDO/HMI data. *Astrophys. Space Sci*. 2018, vol. 363, iss. 3, 61. DOI: 10.1007/s 10509-018-3284-3.

Foullon C., Verwichte E., Nakariakov V.M. Ultra-long-period oscillations in EUV filaments near to eruption: two-wavelength correlation and seismology. *Astrophys. J*. 2009, vol. 700, iss. 2, pp. 1658–1665. DOI: 10.1088/0004-637X/700/2/1658.

Freij N., Dorotovič I., Morton R.J., Ruderman M.S., Karlovský V., Erdélyi R. On the properties of slow MHD sausage waves within small-scale photospheric magnetic structures. *Astrophys. J*. 2016, vol. 817, iss. 1, 44. DOI: 10.3847/0004-637X/817/1/44.

Howard R., Adkins J.M., Boyden J.E., Cragg T.A., Gregory T.S., Labonte B.J. Solar rotation results at Mount Wilson. Part 4: Results. *Solar Phys*. 1983, vol. 83, iss. 2, pp. 321–338.

Kolotkov D.Y., Smirnova V.V., Strekalova P.V., Riehokainen A., Nakariakov V.M. Long-period quasi-periodic oscillations of a small-scale magnetic structure on the Sun. *Astron. Astrophys*. 2017, vol. 598, L2. DOI: 10.1051/0004-6361/201629951.

Newton H.W., Nunn M.L. The Sun's rotation derived from sunspots 1934–1944 and additional results. *Monthly Not. Roy. Astron. Soc*. 1951, vol. 111, iss. 4, pp. 413–421. DOI: 10.1093/mnras/111.4.413.

Scherrer P.H., Schou J., Bush R.I., Kosovichev A.G., Bogart R.S., Hoeksema J.T., Liu Y., Duvall T.L. Jr., Zhao J.,

Title A.M., Schrijver C.J., Tarbell T.D., Tomczyk S. The Helioseismic and Magnetic Imager (HMI) investigation for the Solar Dynamics Observatory (SDO). Solar Phys. 2012, vol. 275, iss. 1–2, pp. 207–227. DOI: 10.1007/s11207-011-9834-2.

Smirnova V.V., Efremov V.I., Parfinenko L.D., Riehokainen A., Solov'ev A.A. Artifacts of SDO/HMI data and long-period oscillations of sunspots. Astron. Astrophys. 2013, vol. 554, A121. DOI: 10.1051/0004-6361/201220825.

Snodgrass H.B. Magnetic rotation of the solar photosphere. Astrophys. J. 1983, vol. 270, pp. 288. DOI: 10.1086/161121.

Solov'ev A.A., Kirichek E.A. Basic properties of sunspots: equilibrium, stability and long-term eigen oscillations. Astrophys. Space Sci. 2014, vol. 352, iss. 1, pp. 23–42. DOI: 10.1007/s10509-014-1881-3.

Tang F. Rotation rate of high-latitude sunspots. Solar Phys. 1981, vol. 69, p. 339.

Thomas J.H., Cram L.E., Nye A.H. Dynamical phenomena in sunspots. I. Observing procedures and oscillatory phenomena. *Astrophys. J.* 1984, vol. 285, pp. 368–385.

Yuan D., Nakariakov V.M., Chorley N., Foullon C. Leakage of long-period oscillations from the chromosphere to the corona. *Astron. Astrophys*. 2011, vol. 533, A116. DOI: 10.1051/0004-6361/201116933.

Zirin H. Astrophysics of the Sun. Cambridge University Press, 1988, 448 p.

How to cite this article

Zhivanovich I., Riehokainen A., Solov'ev A.A., Efremov V.I. Quasi-periodic oscillations of small-scale magnetic structures and a specific method for measuring the differential rotation of the Sun. *Solar-Terrestrial Physics.* 2019. Vol. 5. Iss. 1. P. 3–10. DOI: 10.12737/stp-51201901.